Int J Appl Earth Obs Geoinformation 79 (2019) 110–115

Contents lists available at ScienceDirect

Int J Appl Earth Obs Geoinformation

journal homepage: www.elsevier.com/locate/jag

Remotely sensed vegetation index and LAI for parameter determination of the CSM-CROPGRO-Soybean model when *in situ* data are not available

Jonathan Richetti[a,b,*], Kenneth J. Boote[b], Gerrit Hoogenboom[b,c], Jasmeet Judge[b], Jerry A. Johann[a], Miguel A. Uribe-Opazo[a]

[a] Agricultural Engineering Department, State University of West Parana, Rua Universitaria, 1619, Cascavel, Parana, Brazil
[b] Agricultural & Biological Engineering Department, University of Florida, Frazier Rogers Hall, Gainesville, FL 32611, USA
[c] Institute for Sustainable Food Systems, University of Florida, Frazier Rogers Hall, Gainesville, FL 32611, USA

ARTICLE INFO

Keywords:
Remote sensing
Light interception
Extinction coefficient
Crop model calibration

ABSTRACT

An agricultural system is a complex combination of many different components that require different types of data for analysis and modeling. Remote sensing information is an alternative source of data for areas that only have a small amount of ground truth data. The goal of this study was to evaluate whether remotely sensed data can be used for calibration of genetic specific parameters (GSPs) with the ultimate goal of yield estimation. This study used the Normalized Difference Vegetation Index (NDVI) and Enhanced Vegetation Index (EVI) from Moderate Resolution Imaging Spectroradiometer (MODIS) with measured Leaf Area Index (LAI) for soybean fields in Paraná, Brazil and Iowa, USA, to calibrate the cultivar parameters of the CSM-CROPGRO-Soybean model. Three calibration methods were performed including field-measured LAI, remotely sensed derived LAI, and remotely sensed derived Light Interception. The cultivar parameters sensitive to LAI and LI were calibrated for yield with a mean error of -4.5 kg/ha (0.1%) and with a R^2 of 0.89 for Parana. The availability of crop growth measurements for Iowa resulted in an average RMSE of 895 kg/ha (average *n*RMSE of 6%), and Willmott agreement index of 0.98 for time-series biomass, and an average RMSE of 941 kg/ha (average *n*RMSE of 15%) for pod weight. This study showed that remotely sensed LAI and LI from NDVI data can be used for calibration of GSPs with the ultimate goal of improving yield predictions based on local dynamic temporal and spatial variability.

1. Introduction

Soybean is a major agricultural commodity for Brazil and US in terms of acreage, production, and export. Understanding and estimating how this crop responds to different environmental conditions and crop management practices requires a complex system with combinations of various components that contain a number of interacting biological, physical, and chemical processes (Jones et al., 2017; Tsuji et al., 1998). The Decision Support System for Agrotechnology Transfer (DSSAT) is a suite of software models that simulate such complexity, as it encompasses models for different crops including the CROPGRO model for soybean and other grain legumes (Boote et al., 1998b; Jones et al., 2003; Hoogenboom et al., 2015). For the accurate use of the CROPGRO model for yield prediction, determining the cultivar parameters is essential. Nevertheless, calibration of individual parameters of a crop model may require many experimental datasets and other resources (Fukui et al., 2015; Hoogenboom et al., 2015; Jégo et al., 2010; Jones et al., 2003; Kajumula Mourice et al., 2014; Boote et al., 1998b; Tsuji et al., 1998). Obtaining region- and site-specific *in situ* data that can be used for regional yield estimation is normally challenging because the observed information usually not available, especially for large areas.

Indirect data collection can be conducted to fill possible *in situ* gaps. Because remote sensing data possess a significant potential for monitoring vegetation dynamics (Kasampalis et al., 2018) due to their synoptic coverage and frequent temporal sampling (Atzberger, 2013), such data can be used for modeling purposes. Li et al. (2015) stated that a combination of remote sensing and crop growth models can be an effective tool for grain yield estimation. For example, Chakrabarti et al. (2014) assimilated downscaled remote sensing soil moisture from the Soil Moisture and Ocean Salinity (SMOS) mission into the DSSAT-CROPGRO model using an Ensemble Kalman filter-based augmented state-vector technique that estimates states and parameters simultaneously. This framework was implemented in La Plata basin in Brazil

* Corresponding author at: Agricultural Engineering Department, State University of West Parana, Rua Universitaria, 1619, Cascavel, Parana, Brazil.
E-mail address: jonathan.richetti@unioeste.br (J. Richetti).

https://doi.org/10.1016/j.jag.2019.03.007
Received 1 August 2018; Received in revised form 24 December 2018; Accepted 4 March 2019

for two years and the root mean square error (RMSE) between the assimilated and observed soybean yield were 16.8% during the first growing season and 4.4% during the second season. Fang et al. (2011) integrated the Cropping System Model-CERES-Maize with the MODIS LAI products for estimating corn yield in the state of Indiana, USA, and concluded that the inversion of a crop simulation model facilitates several different user input modes and outputs a series of agronomic and biophysical variables, including crop yield. Campos et al. (2018) developed an operational remote sensing approach to assist crop growth models in reproducing actual processes in the field by relating satellite-based remote sensing data and key canopy biophysical parameters. They proposed a relation-based crop coefficient using field data obtained from 11 years of irrigated and rainfed soybean and maize grown in eastern Nebraska. They concluded that the relationship between biomass production and the reflectance is strong, indicating that the use of remote sensing data for a quantitative analysis of crop biomass production and yield is reliable. Therefore, integrating biophysical data from remotely sensed data could improve the yield prediction of crop simulation models (Doraiswamy et al., 2005). The main advantages from incorporating remote sensing data into crop models are the representation of the missing spatial information and the more accurate description of the crop's actual conditions during various stages of the growing season (Kasampalis et al., 2018). However, remote sensing-based techniques to calibrate crop growth models such as CROPGRO are not fully understood, especially for GSPs, that are critical for predicting crop development and growth and ultimately yield correctly. Using remote sensing to calibrate the model can be an asset for applying the model for gridded applications for large areas and making the use of the model viable when limited observational data are available.

LAI and LI are strong links between remote sensing and the CROPGRO model (Boote et al., 1998a; Hoogenboom et al., 2015). Both can be derived from remote sensing data. As described by Boote et al. (1998a), LAI and LI are state variables because the model simulates LAI over time and uses the LI and subsequent prediction of leaf-to-canopy assimilation, which affects biomass and final yield. Because both LAI and LI are outputs of the model, one can use observed data with model inversion techniques to solve for model parameters that affect LAI and LI. The goal of the study was to understand the utility of remote sensing observations to improve yield predictions from crop growth models. Specific objectives were (1) to test three methods to calibrate the GSPs using field-measured LAI, remote-sensing-derived LAI, and remote-sensing-derived Light Interception (LI), and (2) to compare results with field data to evaluate the feasibility and accuracy of these methods.

2. Materials and methods

2.1. Study area and field data

There were two study areas with an average of 50 ha for each field, including a commercial farm in the western region of Paraná state (southern Brazil) and a commercial farm in the center of Iowa (northern USA). In Brazil, there were two rainfed and two irrigated soybean fields. Crop management for all fields was based on a row spacing of 30 cm for one rainfed and one irrigated field and 45 cm for the other fields. The Brazilian farm is located at 24°42'25.2"S 53°28'48.0"W with humid subtropical climate - Cfa (Aparecido et al., 2016). For the Brazilian fields, weather data were obtained from the European Centre for Medium-Range Weather Forecasts (ECMWF) ERA-Interim data (European Union, 2014), including daily total rainfall, maximum and minimum temperature, dew point temperature, wind speed, and solar radiation. The soil profile was a *Latossolo Vermelho* soil already present in DSSAT. LAI was measured every 16 days using the LI-COR - LAI-2200C Plant Canopy Analyzer during the 2016–2017 growing season (Fig. 1). LAI is the leaf area per unit of land area (Chang, 1968). LAI is used as an indicator of plant growth and for evaluating assimilation and transpiration rates in plant physiological studies. LAI measurements provide indices of plant growth over time and are customarily used as data for calibrating crop simulation models (Hoogenboom et al., 1999). For each field, LAI measurements with six replicates were taken on seven sampling dates. The highest value of LAI occurred in the irrigated field with 45-cm row spacing on December 12, 2016 (75 days after planting). Final yield for each field was measured. Soybean was sown on October 2, 2016 and harvested on February 4, 2017.

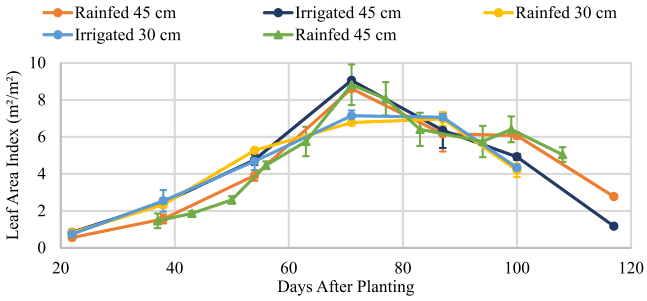

Fig. 1. Measured LAI (m^2/m^2) for the soybean fields in Brazil (solid circles) and US (triangles).

The US field was under rainfed conditions with a 45 cm row spacing. The US farm is located at 42°55'49.9"N 93°22'50.1"W with a humid continental climate – Dfa (Kottek et al., 2006). For this field, the daily weather data were obtained from the Tropical Rainfall Measuring Mission (TRMM) for rainfall, from the Geostationary Operational Environmental Satellite (GOES) for temperature, dew point and wind speed, and from NASA-Prediction of Worldwide Energy Resource (NASA-Power) for solar radiation. The soil was a loam soil already present in DSSAT. Destructive sampling was used to determine the LAI approximately every 6 days with three replicates for each sampling date (Fig. 1). LAI was measured by taking two representative plants in the sampling area and separating the leaves for leaf area determination. The leaves and the rest of the plants were dried at 60 °C for one week to determine the dry weight of the leaf and the dry biomass of the sample that were used to determine LAI. With the specific leaf area and the total dry biomass, LAI was determined (Boote, 1994; Bongiovanni et al., 2015). The highest LAI value was observed on August 26, 2016 (75 days after planting). Sowing and harvest dates, pod weight, and total dry biomass were measured for the USA field. Seed yield was estimated from the final pod mass sampling that was multiplied by published seed-to-pod mass ratio (Dracup and Kirby, 1996; Schobeck et al., 1986; Spaeth and Sinclair, 1985; Batchelor et al., 1994). Soybean was sown on June 12, 2016 and harvested on September 10, 2016.

2.2. Remote sensing data

The EVI and NDVI from the MODIS, products MOD13Q1 (from Terra platform) and MYD13Q1 (from Aqua platform) have a spatial resolution of 250 m and a temporal resolution of 8 days (NASA LP DAAC, 2015). These 8-day composite images are generally very reliable for tracking the changes in vegetation conditions (Kouadio et al., 2014). In addition, LAI from the LAI from the *MODIS/Terra + Aqua Leaf Area Index/FPAR 4-Day L4 Global 500 m SIN Grid V006* (MCD15A3H) with a 500 m spatial resolution and a 4-day temporal resolution were used. MODIS products were extracted for each field, thus creating an EVI, NDVI, and LAI time series for each field. The MODIS products were retrieved online from the Application for Extracting and Exploring Analysis Ready Samples (AρρEEARS), courtesy of the NASA EOSDIS Land Processes Distributed Active Archive Center (LP DAAC), USGS/Earth Resources Observation and Science (EROS) Center (https://lpdaac.usgs.gov).

2.3. Sensitivity analysis of the CSM-CROPGRO-Soybean model

The CSM-CROPGRO-Soybean model computes canopy photosynthesis at hourly time steps using leaf-level photosynthesis parameters, LAI, and hedgerow light interception calculations. Mechanistic responses to weather factors and plant physiological factor-related analysis are possible because of the hourly leaf-level photosynthesis calculations, and realistic responses to row spacing and plant density are due to the hedgerow approach (Boote et al., 1998a). The LAI is part of the canopy architecture and is an important state variable in the CROPGRO module. The module predicts LAI and uses this predicted information for further calculations such as canopy photosynthesis, potential plant transpiration and potential soil water evaporation (Boote et al., 1998a). The CROPGRO-Soybean model has 18 cultivar parameters. A sensitivity analysis was conducted that found five parameters to which LAI and LI were the most sensitive. Subsequently, another analysis was performed to assess the impacts of these five parameters on grain yield. The default Maturity Group 5 was used for Brazil and the default Maturity Group 3 was used for the USA as a starting point for the sensitivity analysis. This was based on the fact that these maturity groups are typical types for the two study areas. We used the DSSAT Cropping System Model Version 4.6.5.001 (Hoogenboom et al., 2015) that includes the CROPGRO-Soybean module.

2.4. Leaf area index and light interception estimations

Based on the Beer–Lambert equation of light extinction (Monsi, 1953) the relationship between remotely sensed MODI EVI, NDVI and LAI with measured LAI was tested. The information from the vegetation indices was used to obtain the remotely sensed derived LAI (RSD-LAI, Eq. (1)) with the extinction coefficient (k) function based on days after planting (DAP). Remotely sensed derived LI (RSD-LI, Eq. (2)) uses RSD-LAI and a single k value to compute LI.

$$RSD\text{-}LAI = -\frac{\ln(1-(VI))}{k} \quad (1)$$

$$RSD\text{-}LI = 1 - exp(-k*RSD - LAI) \quad (2)$$

The effect of drought is presumed to cause a decrease in the extinction coefficient of the canopy because of leaflet tilting and drooping. Similarly, the vegetation indexes decreases under drought effect.

2.5. Calibration methods

In order to evaluate how remotely sensed data can be used for model calibration, three methods were used (Fig. 2). The first calibration (Calibration I) used field-measured LAI as unique temporal data for calibrating the CROPGRO-Soybean cultivar parameters. The second calibration (Calibration II) used RSD-LAI. The third calibration (Calibration III) used RSD-LI. Each calibration was performed using the DSSAT sensitivity analysis tool, which allows for changing a given parameter with small increments, and subsequently computing the statistics of the comparison between simulated and observed data. The following parameters were calibrated; Critical Short Day Length (CSDL - [hours]), which is the day length below which reproductive development progresses with no day length effect for short day plants; time between first flower (R_1) and end of leaf expansion (FL-LF – [photothermal days]); maximum size of full leaf (three leaflets) (SIZLF – [cm^2]); maximum leaf photosynthesis rate at 30 °C, 350 vpm CO_2, and high light (LFMAX – [mg CO_2 $m^{-2}s^{-1}$]); the time required for cultivar to reach final pod load under optimal conditions (PODUR – [photothermal days]). First, CSDL was targeted to the harvest date. Then FL-LF, SIZLF, and LFMAX were targeted to the measured LAI (for Calibration I), RSD-LAI (for Calibration II), and RSD-LI (for Calibration III). Then PODUR was targeted to observed final yield. The mean error

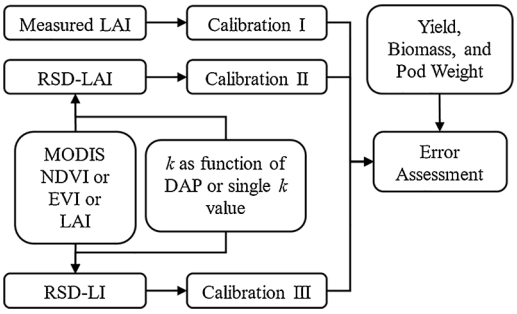

Fig. 2. Study flowchart showing that MODIS NDVI, EVI, and LAI were tested with extinction coefficient (k) based on days after planting (DAP) and single averaged k value for Calibration II and III. By the end and error assessment was performed for 6 remotely sensed derived leaf area index (LAI), namely: RSD-LAI from NDVI with $k = f$(DAP); RSD-LAI from NDVI with single k; RSD-LAI from EVI with $k = f$(DAP); RSD-LAI from EVI with single k; RSD-LAI from MODIS LAI. Same for remotely sensed derived light interception (LI). This process was performed for each studied field.

(ME), mean absolute error (MAE), root mean square error (RMSE), normalized root mean square error (nRMSE) and coefficient of determination (R^2) were used to assess the different yield estimations. In addition, the Willmott agreement index (d; Willmott, 1981) was used for determining the accuracy of pod weight and biomass time series simulations.

3. Results and discussion

3.1. LAI and LI estimations

The extinction coefficient (k) was either based on a function of days after planting (DAP) or on a single fixed value as discussed in the methods. From the vegetation indices that were tested, including MODIS NDVI, EVI and MODIS LAI *vs* measured data, the best results were obtained with RSD-LAI from NDVI. Field measured LAI and NDVI were used to solve k values for each date with Eq. (1). Because the k values changed with time, Eqs (3) and (4) represent k value as a function of DAP, for Brazil and USA, respectively. Both equations had R^2 above 0.7 and were used to estimate LAI dependent on NDVI without the need for field data. Slightly different coefficients may result from slower rate of LAI development, associated with cooler weather in Iowa, USA.

$$k = 68.623 * DAP^{-1.170} (R^2 = 0.71) \quad (3)$$

$$k = 52.062 * DAP^{-1.215} (R^2 = 0.75) \quad (4)$$

Similarly, the remotely sensed derived LI (RSD-LI) was estimated using a type of light interception equation (Eq. (2)). For RSD-LAI and RSD-LI the extinction coefficient value (k) was tested based on the days after planting function and on a single value. However, for the RSD-LI estimations a fixed extinction coefficient value ($k = 0.7063$, derived from CROPGRO-Soybean) gave better results than using variable extinction coefficient equations as was used for RSD-LAI.

3.2. Crop model cultivar parameter calibration

The measured LAI, RSD-LAI, and RSD-LI were added to the DSSAT software as time-series data for a comparison between simulations and observations. A sensitivity analysis was performed comparing the simulated LAI or LI with the measured LAI, RSD-LAI, or RSD-LI. The RMSE and d were used to define the best values for the cultivar parameters. Because CSDL is sensitive to crop cycle and the harvest date was the same for all Brazilian fields (Feb 4), all calibration methods presented similar harvest date simulations. Using LAI as target, FL-LF, SIZFL, and LFMAX were calibrated, obtaining the same results for

Table 1
Cultivar parameters determined based on calibration approaches.

	cycle	- - - -Solving for LAI/LI - - -			- Yield -
Calibration	CSDL[a]	FL-LF[b]	SIZLF[b]	LFMAX[b]	PODUR[c]
Brazilian field					
Default Maturity Group 5	12.83	18	180	1.03	10
Calibration I (Measured LAI)	12.68	34	230	1.20	26
Calibration II (RSD-LAI from NDVI)	12.68	34	230	1.20	26
Calibration III (RSD-LI from EVI)	12.68	26	230	1.03	31
Calibration I (from MG 6)	13.14	34	230	1.20	26
US field					
Default Maturity Group 3	13.40	26	180	1.03	10
Calibration I (Measured LAI)	13.98	34	230	1.20	28
Calibration II (RSD-LAI from NDVI)	13.98	34	230	1.20	28
Calibration III (RSD-LI from EVI)	13.98	26	230	1.03	25

[a] Targeted to the harvest date.
[b] Targeted to the LAI or LI.
[c] Targeted to yield.

calibration I and II (measured LAI and RSD-LAI from NDVI, respectively), but different results were obtained for calibration III (with RSD-LI from EVI). To determine the sensitivity to the initial values for the cultivar parameters, the Generic Maturity Group 6 cultivar was used as a starting point. However, the values for the cultivar parameters FL-LF, SIZLF, and LFMAX converged to similar values (Table 1).

The solved parameters indicate that the cultivar used in Parana is an indeterminate cultivar, because FL-LF and PODUR resulted in higher values, indicating an extended period of leaf area growth and pod addition after the beginning of flowering. LAI and LI are sensitive to the parameters LF-FL, SIZLF, and LFMAX. Other parameters were not appropriate to calibrate against LAI because those parameters either did not create differences in LAI or LI as the selected output targets or, as in the case for CSDL, were tightly related to the life cycle which should be calibrated independently against final harvest or the end-of-season decline in LAI. This is similar to Dzotsi et al. (2013) who found that the SALUS crop model in DSSAT was not sensitive to parameters associated with the prediction of the timing of germination and emergence, but the most influential parameters were related to LAI growth, crop duration, and thermal time accumulation. In addition, remote sensing images are based on light interception, transmission and reflectance characteristics of crop canopies, thus using such information to determine light interception is conceptually closer to light interception predicted by the model than to crop LAI (a biological characteristic predicted by the model). Therefore, CSDL can be calibrated based on development cycle data, FL-LF, SIZLF, and LFMAX can be calibrated using measured LAI, RSD-LAI or RSD-LI, and PODUR can be calibrated with final yield. This means that non-destructive methods can be used for model calibration.

Table 3
Statistics for yield estimations (kg/ha) based on calibration approaches: measured LAI (Calibration I), remotely sensed derived LAI (Calibration II) or remotely sensed derived LI (Calibration III).

	No Calibration	Calibration I	Calibration II	Calibration III
ME	20.4	−5.0	−5.0	−3.4
MAE	264.8	145.0	145.0	133.8
RMSE	341.6	213.9	213.9	191.5
*n*RMSE	8.3%	5.2%	5.2%	4.7%
R^2	0.60	0.85	0.85	0.89

*No calibration means that the default maturity group 5 was used.

Table 4
Biomass and pod weight (kg/ha) statistics for each calibration approach: measured LAI (Calibration I), remotely sensed derived LAI (Calibration II) or remotely sensed derived LI (Calibration III), in the USA field.

	Biomass				Pod Weight			
	No Cal.	Cal. I	Cal. II	Cal. III	No Cal.	Cal. I	Cal. II	Cal. III
ME	−1082	−553	−553	−684	−870	−604	−604	−556
MAE	1082	573	573	706	870	607	607	559
RMSE	1366	864	864	957	1180	960	960	904
*n*RMSE	27%	17%	17%	19%	72%	58%	58%	55%
d	0.95	0.98	0.98	0.98	0.81	0.87	0.87	0.89

3.3. Evaluating the different calibration approaches for effect on yield

Different calibration methods resulted in different values for simulated yield (Table 992). Since calibration I and II produced the same parameters, the results were exactly the same. Therefore, using measured LAI or RSD-LAI from NDVI gave the same results which is a good outcome indicating the value of estimating LAI and yield from remote sensing. In the US field, there was no measurement for yield, so the grain yield was based on the pod weight considering a threshing percentage of 69%. The 69% value was determined from the average of measured threshing percentage from two Iowa experiments (in 1988 and 1990) and two Ohio experiments (in 1988 and 1990) that are included in the distribution version of DSSAT (Hoogenboom et al., 2015). This approach is justified because the seed-to-pod mass ratio is a stable trait for soybean despite considerable yield variation (Dracup and Kirby, 1996; Schobeck et al., 1986; Spaeth and Sinclair, 1985; Batchelor et al., 1994).

Using the calibration methods described previously, the cultivar parameters sensitive to LAI and LI could be calibrated with a mean error of −4.5 kg/ha (0.1%), R^2 of 0.86, and average RMSE of 206 kg/ha (nRMSE of 5%) for all studied fields (Table 3). The availability of crop growth measurements for Iowa, USA, resulted in an average RMSE of 895 kg/ha (average *n*RMSE of 17.7%), and Willmott agreement index of 0.98 for time-series biomass, and an averaged RMSE of 941 kg/ha (average *n*RMSE of 57%), and Willmott agreement index of 0.87 for time-series pod weight (Table 4). Based on the results from the soybean fields in Brazil and the USA, using remote sensing data (Calibration II

Table 2
Actual yield (kg/ha) and model-simulated yields based on three calibration approaches where the calibration was based on measured LAI (Calibration I), remotely sensed derived LAI (Calibration II) or remotely sensed derived LI (Calibration III), followed by a yield calibration.

Field	Actual Yield	Est. Yield No Calibration*	Est. Yield Calibration I	Est. Yield Calibration II	Est. Yield Calibration III
Rainfed 30 cm	4166	3795	4127	4127	4136
Rainfed 45 cm	3771	3750	4112	4112	4074
Irrigated 30 cm	4826	4607	4493	4493	4526
Irrigated 45 cm	*4473*	*4562*	*4470*	*4470*	*4460*
Iowa field	*3295*	*3919*	*3304*	*3304*	*3318*

* No calibration means that the default maturity group 5 was used.

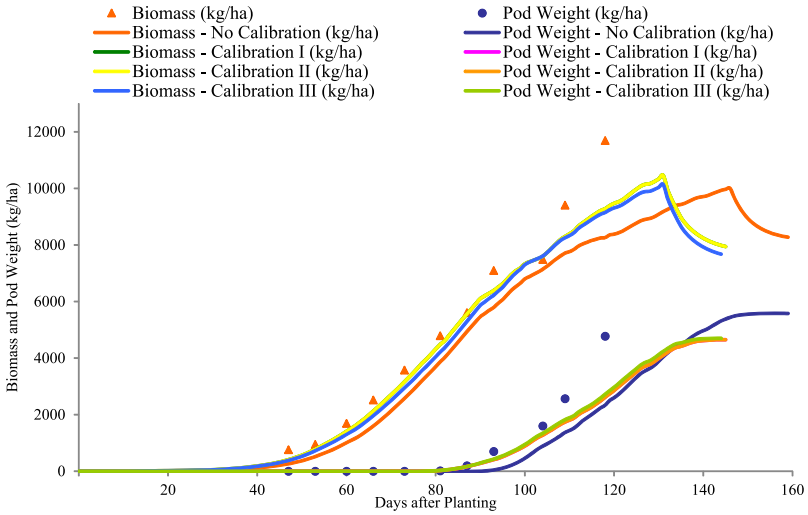

Fig. 3. Biomass and pod weight (kg/ha) time series observations and simulations based on the calibration methods for the US field. Note: Calibration I does not show separately because simulations were identical to those for Calibration II.

and III) had similar results as using measured data (Calibration I) and better results than the unconstrained model (Table 3). Because Calibration III derives from the same data (RSD-LAI to RSD-LI), it has an advantage for those modelers who wish to calibrate their model to LI rather than LAI.

Identifying appropriate experimental and field data for model calibration is a challenge (Hunt et al., 2001; Hoogenboom et al., 2012; White et al., 2013). Mourice et al. (2014) pointed that the lack of experimental data has limited some crop model applications with DSSAT and other modeling platforms. The calibration methods presented in this study can be used to calibrate the cultivar parameters of the CSM-CROPGRO-Soybean model and similar models for other grain legumes easily with RSD-LAI and with less data. This corroborates with Bao et al. (2017) who compared the performance of the CSM-CERES-Maize and EPIC models and concluded that limited data sets from maize variety trials can be used for model calibration when detailed data from growth analysis studies are not readily available. The Calibration III method using the RSD-LI gave the lowest errors for yield for the Brazilian field and lowest errors for biomass and pod weight for the US field. Using this type of approach will make the models more useful for yield forecasting for larger regions where on-the-ground field measures are nonfeasible or not available and remote sensing data can be easily acquired. Effects of calibration methodology can be visualized by evaluating the time course of the simulated biomass and pod mass over time. There were no biomass and pod weight measurements for the Brazilian fields, while for the US field it was possible to confirm that using RSD data such as LAI and LI resulted in achieving good calibration of total biomass and pod weight compared to observed growth (Fig. 3).

For pod weight and biomass prediction, the use of remote sensing data (RSD-LAI or RSD-LI) produce results as good as *in situ* data and better when compared to the unconstrained model (Table 4).

4. Conclusions

This study showed that remote sensing data is a feasible alternative when *in situ* data are not available for model calibration. Using remotely sensed derived LAI or LI from vegetation indices presented similar results as the use of measured LAI and better results than the unconstrained model.

Disclosure

No potential conflict of interest was reported by the authors.

Acknowledgments

This work was supported by the CAPES foundation (Coordination for the Improvement of Higher Education Personnel – Ministry of Education – Brazil) under Grant 88881. 131979/2016-01. The authors are grateful to the farmers for sharing their data.

References

Aparecido, L.E.O., Rolim, G.S., Richetti, J., de Souza, P.S., Johann, J.A., 2016. Köppen, Thornthwaite and Camargo climate classifications for climatic zoning in the State of Paraná, Brazil. Ciencia e Agrotecnologia 40 (4). https://doi.org/10.1590/1413-70542016404003916.

Atzberger, C., 2013. Advances in remote sensing of agriculture: context description, existing operational monitoring systems and major information needs. Remote Sens. 5, 949–981. https://doi.org/10.3390/rs5020949.

Bao, Y., Hoogenboom, G., McClendon, R., Vellidis, G., 2017. A comparison of the performance of the CSM-CERES-Maize and EPIC models using maize variety trial data. Agric. Syst. 150, 109–119. https://doi.org/10.1016/J.AGSY.2016.10.006.

Batchelor, W.D., Jones, J.W., Boote, K.J., Hoogenboom, G., 1994. Carbon-based model to predict peanut pod detachment. Trans. ASAE 37 (5), 1639–1646. https://doi.org/10.13031/2013.28251.

Bongiovanni, T., Liu, P.W., Nagarajan, K., Preston, P., Rush, P., van Emmerik, T.H.M., Terwilleger, R., Monsivais-Huertero, A., Judge, J., Steele-Dunne, S., De Roo, R., Akbar, R., Baar, E., Wallace, M., England, A., 2015. AE514 - Field Observations during the Eleventh Microwave Water and Energy Balance Experiment (MicroWEX-11). University of Florida, pp. 96. from April 25, 2012, through December 6, 2012 IFAS. http://edis.ifas.ufl.edu.

Boote, K.J., 1994. Data requirements for model evaluation and techniques for sampling crop growth and development. In: In: Hoogenboom, Gerrit, Wilken, Paul W., Tsuji, Gordon Y. (Eds.), DSSAT Version 3.5 Vol. 4. University of Hawaii, Honolulu, pp. 215–220.

Boote, K.J., Jones, J.W., Hoogenboom, G., 1998a. Simulation of crop growth: CROPGRO model. Agricultural Systems Modeling and Simulation, 1st ed. CRC Press, pp. 728.

Boote, K.J., Jones, J.W., Hoogenboom, G., Pickering, N.B., 1998b. The CROPGRO model for grain legumes. Understanding Options for Agriculutral Production, 1st ed. Kluwer Academic, Dordrecht, pp. 99–128.

Campos, I., Neale, C.M.U., Arkebauer, T.J., Suyker, A.E., Gonçalves, I.Z., 2018. Water productivity and crop yield: a simplified remote sensing driven operational approach. Agric. For. Meteorol. 249, 501–511. https://doi.org/10.1016/J.AGRFORMET.2017.07.018.

Chakrabarti, S., Bongiovanni, T., Judge, J., Zotarelli, L., Bayer, C., 2014. Assimilation of SMOS soil moisture for quantifying drought impacts on crop yield in agricultural regions. IEEE J. Selected Top. Appl. Earth Obs. Remote. Sens. 7 (9), 3867–3879. https://doi.org/10.1109/JSTARS.2014.2315999.

Chang, Jen-Hu, 1968. Climate and Agriculture: an Ecological Survey, 1st ed. Aldine Publishing Co., Chicago, pp. 304.

Doraiswamy, P.C., Sinclair, T.R., Hollinger, S., Akhmedov, B., Stern, A., Prueger, J., 2005. Application of MODIS derived parameters for regional crop yield assessment. Remote Sens. Environ. 97 (2), 192–202. https://doi.org/10.1016/j.rse.2005.03.015.

Dracup, M., Kirby, E.J.M., 1996. Pod and seed growth and development of narrow-leafed lupin in a water limited mediterranean-type environment. Field Crops Res. 48 (2–3), 209–222. https://doi.org/10.1016/S0378-4290(96)00040-8.

Dzotsi, K.A., Basso, B., Jones, J.W., 2013. Development, uncertainty and sensitivity

analysis of the simple SALUS crop model in DSSAT. Ecol. Modell. 260, 62–76. https://doi.org/10.1016/J.ECOLMODEL.2013.03.017.
European Union, 2014. EC-JRC-MARS Data Created by MeteoConsult Based on ECWMF (European Centre for Medium Range Weather Forecasts) Model Outputs. Retrieved August 19, 2015, from. http://spirits.jrc.ec.europa.eu/?page_id=2869.
Fang, H., Liang, S., Hoogenboom, G., 2011. Integration of MODIS LAI and vegetation index products with the CSM–CERES–Maize model for corn yield estimation. Int. J. Remote Sens. 32 (4), 1039–1065. https://doi.org/10.1080/01431160903505310.
Fukui, S., Ishigooka, Y., Kuwagata, T., Hasegawa, T., 2015. A methodology for estimating phenological parameters of rice cultivars utilizing data from common variety trials. J. Agric. Meteorol. 71 (2), 77–89. https://doi.org/10.2480/agrmet.D-14-00042.
Hoogenboom, G., Wilken, P.W., Tsuji, G.Y., 1999. In: In: Hoogenboom, Gerrit, Wilken, Paul W., Tsuji, Gordon Y. (Eds.), DSSAT Version 3.5 Vol. 4. University of Hawaii, Honolulu, pp. 215–220.
Hoogenboom, G., Jones, J.W., Traore, P.C.S., Boote, K.J., 2012. Experiments and data for model evaluation and application. In: Kihara, J., Fatondji, D., Jones, J.W., Hoogenboom, G., Tabo, R., Bationo, A. (Eds.), Improving Soil Fertility Recommendations in Africa Using the Decision Support Systems for Agrotechnology Transfers (DSSAT). Springer, Dordrecht, the Netherlands, pp. 9–18.
Hoogenboom, G., Jones, J.W., Wilkens, P.W., Porter, C.H., Boote, K.J., Hunt, L.A., et al., 2015. Decision Support System for Agrotechnology Transfer (DSSAT) Version 4.6. Retrieved from. DSSAT Foundation, Washington. www.DSSAT.net.
Hunt, L.A., White, J.W., Hoogenboom, G., 2001. Agronomic data: advances in documentation and protocols for exchange and use. Agric. Syst. 70, 477–492.
Jégo, G., Bourgeois, G., Morrison, M.J., Drury, C.F., Tramblay, N., Tramblay, G., 2010. Calibration and performance evaluation of soybean and spring wheat cultivars using the STICS crop model in Eastern Canada. Field Crops Res. 117, 183–196. https://doi.org/10.1016/j.fcr.2010.03.008.
Jones, J.W., Hoogenboom, G., Porter, C.H., Boote, K.J., Batchelor, W.D., Hunt, L.A., et al., 2003. The DSSAT cropping system model. J. Agron. 18, 235–265. Retrieved from. www.elsevier.com/locate/eja.
Jones, J.W., Antle, J.M., Basso, B., Boote, K.J., Conant, R.T., Foster, I., et al., 2017. Brief history of agricultural systems modeling. Agric. Syst. 155, 240–254. https://doi.org/10.1016/J.AGSY.2016.05.014.
Kajumula Mourice, S., Rweyemamu, C.L., Tumbo, S.D., Amuri, N., Mourice, S.K., 2014. Maize cultivar specific parameters for decision support system for agrotechnology transfer (DSSAT) application in Tanzania. Am. J. Plant Sci. 5 (5), 821–833. https://doi.org/10.4236/ajps.2014.56096.
Kasampalis, D., Alexandridis, T., Deva, C., Challinor, A., Moshou, D., Zalidis, G., 2018. Contribution of remote sensing on crop models: a review. J. Imaging 4 (4), 52. https://doi.org/10.3390/jimaging4040052.
Kottek, M., Grieser, J., Beck, C., Rudolf, B., Rubel, F., 2006. World Map of the Köppen-Geiger climate classification updated. Meteorol. Z. 15 (3), 259–263. https://doi.org/10.1127/0941-2948/2006/0130.
Kouadio, L., Newlands, N.K., Davidson, A., Zhang, Y., 2014. Assessing the Performance of MODIS NDVI and EVI for Seasonal Crop Yield Forecasting at the Ecodistrict Scale (i). pp. 10193–10214. https://doi.org/10.3390/rs61010193.
Li, Z., Jin, X., Zhao, C., Wang, J., Xu, X., Yang, G., et al., 2015. Estimating wheat yield and quality by coupling the DSSAT-CERES model and proximal remote sensing. Eur. J. Agron. 71, 53–62. https://doi.org/10.1016/j.eja.2015.08.006.
Monsi, M., 1953. Uber den Lichtfaktor in den Pflanzengesellschaften und seine Bedeutung fur die Stoffproduktion. Jpn. J. Bot. 14, 22–52.
NASA LP DAAC, 2015. MODIS Products Table. Retrieved May 14, 2015, from. https://lpdaac.usgs.gov/products/modis_products_table.
Schobeck, M.W., Hsu, F.C., Carlsen, T.M., 1986. Effect of pod number on dry matter and nitrogen accumulation and distribution in soybean. Crop Sci. 26 (4), 783. https://doi.org/10.2135/cropsci1986.0011183X002600040033x.
Spaeth, S.C., Sinclair, T.R., 1985. Linear increase in soybean harvest index during seed-filling1. Agron. J. 77 (2), 207. https://doi.org/10.2134/agronj1985.00021962007700020008x.
Tsuji, G.Y., Hoogenboom, G., Thornton, P., 1998. In: Tsuji, G.Y., Hoogenboom, G., Thornton, P. (Eds.), Understanding Options for Agricultural Production, Retrieved from. http://www.springer.com/gp/book/9780792348337#aboutBook.
White, J.W., Hunt, L.A., Boote, K.J., Jones, J.W., Koo, J., Kim, S., Porter, C.H., Wilkens, P.W., Hoogenboom, G., 2013. Integrated description of agricultural field experiments and production: the ICASA Version 2.0 data standards. Comput. Electron. Agric. 96 (1), 1–12.
Willmott, C.J., 1981. On the validation of models. Phys. Geogr. 2 (2), 184–194. https://doi.org/10.1080/02723646.1981.10642213. Retrieved from:.